

# Confidence-Calibrated Face and Kinship Verification

Min Xu, Ximiao Zhang, and Xiuzhuang Zhou

**Abstract**—In this paper, we investigate the problem of predictive confidence in face and kinship verification. Most existing face and kinship verification methods focus on accuracy performance while ignoring confidence estimation for their prediction results. However, confidence estimation is essential for modeling reliability in such high-risk tasks. To address this issue, we first introduce a simple yet effective confidence measure for face and kinship verification, which allows the verification models to transform the similarity score into a confidence score for a given face pair. We further propose a confidence-calibrated approach called angular scaling calibration (ASC). ASC is easy to implement and can be directly applied to existing face and kinship verification models without model modifications, yielding accuracy-preserving and confidence-calibrated probabilistic verification models. To the best of our knowledge, our approach is the first general confidence-calibrated solution to face and kinship verification in a modern context. We conduct extensive experiments on four widely used face and kinship verification datasets, and the results demonstrate the effectiveness of our approach. Code and models are available at <https://github.com/cnulab/ASC>.

**Index Terms**—Kinship verification, face verification, confidence estimation, confidence calibration, angular scaling.

## I. INTRODUCTION

Face and kinship verification are two popular facial analysis tasks in computer vision. Face verification attempts to determine whether or not a given pair of face samples belong to the same subject [1]. Kinship verification aims to predict whether or not there is a kin relation between a given pair of face samples [2]. Face and kinship verification tasks based on deep learning technologies have achieved remarkable performance under controlled conditions in the past decade. However, the two tasks in the wild are still challenging due to large intra-class variations, such as complex background, occlusion, and a variety of variations on illumination, pose and facial expression. Prior works on face and kinship verification are generally devoted to improve prediction accuracy, while paying little attention to confidence estimation. We argue that the reliability is also a key measure for evaluating the performance of these verification algorithms, and it becomes even more crucial for those verification systems deployed in high-risk scenarios. In this paper, we focus on modeling confidence estimation and calibration for face and kinship verification.

Accurate confidence estimation for face and kinship verification is often difficult. One reason can be that the labels describing sample (pairs) uncertainty are usually not offered in most face or kinship verification datasets. To address this issue, existing approaches often tend to train a separate network [3] or an extra network branch [4]–[6] to model data uncertainty. However, they are devoted to uncertainty estimation of individual face images rather than confidence estimation for given face pairs. On the other hand, modern neural networks tend

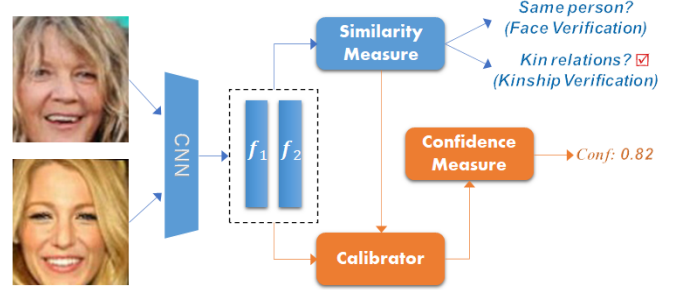


Fig. 1. The pipeline of our proposed confidence-calibrated face and kinship verification. Different from previous methods, our method gives additional well-calibrated confidence estimation on the prediction, by introducing a simple confidence measure and a flexible calibrator that can be directly applied to most existing face and kinship verification models without modifications.

to be over- or under-confident in their predictions. Hence, the similarity score of a face pair may not correctly reflect the verification confidence. For these reasons, in this paper we propose a simple yet effective confidence measure for face and kinship verification. Our approach is inspired by the following observation: If the pair similarity is close to the decision threshold  $\tau$ , the model is less likely to make a correct prediction. On the other hand, if the pair similarity is far from the threshold, the model’s prediction is more likely to be correct. The proposed measure allows face and kinship verification models to transform the similarity score into a confidence score for a given face pair. We further develop a new algorithm to adjust the similarity of face pairs in angular space, so that the calibrated confidence can well quantify the predictive confidence while maintaining the verification accuracy.

The pipeline of our confidence-calibrated face and kinship verification is illustrated in Fig. 1. The main contributions of this work can be outlined below:

- 1) We introduce a new confidence measure for probabilistic face and kinship verification, allowing any off-the-shelf verification models to efficiently estimate the prediction confidence.
- 2) We develop a confidence-calibrated algorithm via angle scaling, which can be directly applied to existing face and kinship verification models without model modifications. To the best of our knowledge, this is the first general confidence-calibrated solution to face and kinship verification in modern context.
- 3) Extensive experiments are conducted on both face and kinship datasets, and the results demonstrate that our proposed method achieves state-of-the-art calibration performance.

The rest of the paper is organized as follows. In section II, we first review prior works on face and kinship verification,

and then discuss related works on confidence estimation in face analysis. In section III, we elaborate our proposed confidence measure for face and kinship verification, followed by our confidence-calibrated approach. In section IV, we present experimental results and analysis. Finally, we conclude the paper in section V.

## II. RELATED WORKS

### A. Face and Kinship Verification

Face verification is a well-studied research topic in computer vision. In early studies, the low-level handcrafted features were used for verification and identification. The development of deep neural networks in the past decade has greatly improved the performance of face verification. DeepFace [7] and DeepID [8] were the earlier studies to introduce deep CNNs into face recognition, which explored deep models to learn effective high-level features, thus boosting the face recognition performance. FaceNet [9] proposed the triplet loss to learn a direct mapping from face images to a compact Euclidean space, with distances directly related to a measure of face similarity. Wen et al. [10] proposed a center loss to enhance the compactness of intra-class samples by minimizing the Euclidean distance between deep feature vectors and their corresponding class centers, while combining a softmax loss to guarantee inter-class differences. Large-Margin Softmax [11] inspired new ideas for face verification tasks, and many excellent studies have emerged since then, such as SpereFace [12], CosFace [13], and ArcFace [14]. These methods penalised the angles between deep features and their corresponding weights in angular space, which improved effectively the discriminative ability of feature embeddings. Note that vector angular-based distance measure has gradually replaced the Euclidean distance measure as the most popular method for face verification tasks, since the cosine of the angle and the Softmax loss are inherently consistent.

The facial kinship verification problem can be dated back to the pioneering work by Fang et al. [2]. Since then, a variety of approaches have been proposed [15]. These approaches can be roughly divided into two categories: one is the traditional methods based on feature or metric learning, and the other is the deep learning-based approaches developed in recent years. The former seeks to learn a feature encoder or distance metric from pairwise kinship samples, and the representative work of this line is the neighborhood repulsed metric learning (NRML) [16], with the goal of learning a distance metric that maximizes the distance between negative pairs while minimizing the distance between positive pairs. Following this, [17]–[22] expanded on this concept by developing the novel approaches combining multiple features [17], [20], multiple views [19]–[21], multiple similarity [18], [21], and denoising [22]. Recently, research works [23]–[34] based on traditional methods have been renovated with deep learning techniques, such as deep metric learning, deep feature representation, or their combination to solve the kinship recognition problem [23], [26], [29], [30]. Besides that, a variety of kinship recognition solutions with generative modeling [35]–[37] or graph

representation [38] have been developed to further improve the robustness of the kinship verification.

As discussed above, most existing face and kinship verification methods focus on accuracy performance, while ignoring the confidence estimation for their predictions. Even though a few attempts have been made recently to estimate the prediction confidence [39], the estimated confidence can be inaccurate due to the poor calibration of modern DNNs [40]. Differently, our method provides well-calibrated predictive confidence while maintaining the verification accuracy.

### B. Uncertainty and Confidence Estimation in Face Analysis

In recent years, a variety of computer vision tasks, ranging from object detection [41], semantic segmentation [42], to image retrieval [43], [44], have introduced uncertainty estimation into deep models to improve the robustness and interpretability of the system. Uncertainty can generally be classified into two types: aleatoric uncertainty and epistemic uncertainty [45]. The former relates to the noise-related uncertainty in the data, whereas the latter relates to the parameter uncertainty in the prediction model. Gal and Ghahramani [46] proposed to model predictive uncertainty by dropout training in deep neural networks as approximate Bayesian inference. Kendall and Gal [45] designed a Bayesian deep learning framework that combines input-dependent aleatoric uncertainty with epistemic uncertainty. Guo et al. [40] investigated various factors affecting the uncertainty of deep models, and evaluated the performance of multiple calibration methods for classification tasks.

There are a few works on the uncertainty analysis in face and kinship verification. Xie et al. [3] proposed to train an independent network to measure the quality of face images. Shi et al. [5] proposed to learn the variance of feature embedding, and measure the likelihood of face pair belonging to the same latent distribution. In [6], the relative uncertainty of face pair is learned through an additional network branch, and the uncertainty is used as a weight to fuse the features with two different labels. In addition, various attempts have been made to incorporate uncertainty analysis into the process of face representation learning [4], [47].

Existing methods for modeling uncertainty in facial feature learning can only provide a uncalibrated uncertainty estimation in the prediction stage, which does not reflect the probability of the prediction being correct. For verification tasks, the confidence measure and calibration approach we proposed can provide well-calibrated prediction confidence in the decision-making process, which directly represents the probability that the prediction is correct and aids in risk assessment. The most closely related work to ours is the approach proposed in [39], where uncertainty of the similarity score is estimated and propagated to the predictive confidence in face verification. However, this approach doesn't take into account the confidence calibration, leading to inaccurate confidence estimation. Experiment results on four widely-used datasets demonstrate that our proposed post-calibration method works well in face and kinship verification in terms of the uncertainty metric.



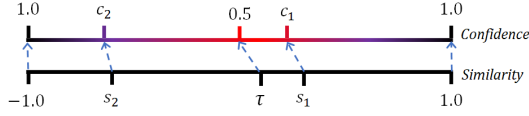


Fig. 2. An illustration for the relation between similarity score and predictive confidence. The closer to the decision threshold  $\tau$  the similarity score  $s$  is, the lower the confidence  $c$  becomes.

### III. OUR APPROACH

#### A. Preliminaries: Face and Kinship Verification

Given a face pair  $(X_1, X_2)$ , existing face and kinship verification methods typically compute a cosine similarity  $s(X_1, X_2) = \frac{\langle f(X_1), f(X_2) \rangle}{\|f(X_1)\| \|f(X_2)\|}$  and then use a decision threshold  $\tau$  for final prediction, where  $f(\cdot)$  is the feature embedding often represented by modern DNNs. Formally, prediction function  $g$  for face and kinship verification can be defined by:

$$g(s, \tau) = \begin{cases} 1, & s \geq \tau \\ -1, & s < \tau \end{cases} \quad (1)$$

where  $\tau$  is a predefined threshold, and often, it is empirically set based on the ROC curve on a held-out validation set.

Recent works on face or kinship verification show that verification systems built even on popular DNNs may not work reliably, especially when the face images are partially occluded or are of low resolution. Therefore, confidence estimation for face and kinship verification plays a key role in such a safety-critical task. However, most existing verification methods based on similarity measure fail to quantify the prediction confidence of face pairs, as the similarity score itself does not exactly reflect the prediction confidence. To address this issue, we propose a simple and flexible confidence measure to quantify the predictive confidence of any face and kinship verification models. Specifically, we estimate the predictive confidence based on the similarity  $s$  and threshold  $\tau$ , and then calibrate the confidence in angular space so that the calibrated confidence relates directly to the probability of the prediction being correct.

#### B. Confidence Measure

Intuitively, if the similarity score of a face pair is equal to the left or right boundary values (-1 or 1), the predictive confidence will reach its maximum value of 1. Obviously, the predictive confidence relates not only to the similarity score but also to the decision threshold.

To model the relation between the similarity score and the predictive confidence for verification problems, we first define a confidence function  $\varphi(s, \tau)$  based on the similarity  $s$  and threshold  $\tau$ :

$$\varphi(s, \tau) = \begin{cases} \frac{s - \tau}{1 - \tau}, & g(s, \tau) = 1 \\ \frac{\tau - s}{1 + \tau}, & g(s, \tau) = -1 \end{cases} \quad (2)$$

where  $s \in [-1, 1]$ , and  $\tau \in (-1, 1)$ . The similarity threshold  $\tau$  divides the cosine similarity interval  $[-1, 1]$  into the positive part and negative part, with size of  $1 - \tau$  and  $1 + \tau$ , respectively, as shown in Fig. 2.

Note that face or kinship verification is a binary decision problem. Hence, the probabilistic confidence  $c$  for a prediction  $g$  based on Eq. (1) should be greater or equal to 0.5. As such, the confidence measure  $c(s, \tau)$  on the prediction  $g$  can be written by:

$$c(s, \tau) = \frac{1}{2} \varphi(s, \tau) + \frac{1}{2} \quad (3)$$

As shown in Fig. 2, if  $s$  takes the value farther away from  $\tau$  (e.g.,  $s = s_2$ ), the predictive confidence  $c$  becomes much higher (e.g.,  $c = c_2$ ). On the contrary, if the value of  $s$  is closer to  $\tau$  (e.g.,  $s = s_1$ ), the confidence  $c$  becomes lower (e.g.,  $c = c_1$ ), indicating the more likely the model makes incorrect predictions. So far, we have propose a flexible confidence measure that can be directly applied to any off-the-shelf verification models to yield a probabilistic estimation of prediction confidence.

#### C. Confidence Calibration via Angular Scaling

In actuality, there is a bias between the verification accuracy and predictive confidence in face and kinship verification problems. This can be due to the fact that modern DNNs are often miscalibrated [40]. The proposed confidence measure may not produce well-matched confidence to the expected accuracy of the model. In classification tasks, it is common to calibrate the model by scaling the *logit* [40]. However, if a similar process is used to directly scale the similarity  $s$  in the verification task, the similarity  $s$ , the threshold  $\tau$ , and the similarity interval will be scaled equally, resulting in no change to the prediction confidence according to Eq. (2). Inspired by the work of [12]–[14], we propose a post-calibration method via angular scaling, which can well calibrate the prediction confidence without retraining the model.

We propose to calibrate the prediction confidence by calibrating the angle  $\theta$  between pairs of face on a recalibration dataset  $D_c = \{(X_i, Z_i), y_i\}_{i=1}^N$ , and a feature encoder denoted as  $f(\cdot)$ . For a sample pair  $(X_i, Z_i)$  with label  $y_i \in \{-1, 1\}$  in  $D_c$ , its feature representation and cosine similarity are denoted by  $x_i = f(X_i)$ ,  $z_i = f(Z_i)$ , and  $s(x_i, z_i)$ , respectively. Our angular scaling calibration (ASC) method learns to adjust the angle between the face pairs based on the similarity set  $S_c = \{s(x_i, z_i)\}_{i=1}^N$  and its labels  $Y_c = \{y_i\}_{i=1}^N$  (derived from the recalibration set  $D_c$ ). Let  $\theta_i$  denote the angle between the two face representation features  $x_i$  and  $z_i$ :

$$\theta_i = \arccos(s(x_i, z_i)) \quad (4)$$

Our ASC learns to adjust the angle  $\theta_i$  using two learnable scalar parameters  $w$  and  $b$ :

$$\theta'_i = \theta_i * w + b \quad (5)$$

where  $w > 0$  and  $\theta'_i \in [0, \pi]$ , and the calibrated similarity is:

$$s'(x_i, z_i) = \cos(\theta'_i) \quad (6)$$

Accordingly, the calibrated threshold will be:

$$\tau' = \cos(\arccos(\tau) * w + b) \quad (7)$$

To learn the calibration parameter  $w$  and  $b$ , we minimize the following objective function:

$$L = \frac{1}{N} \sum_{i=1}^N (s'(x_i, z_i) - y_i)^2 \quad (8)$$

where  $y_i = 1$  if  $(x_i, z_i)$  is a positive pair, and  $y_i = -1$  otherwise.

The detail of the calibration procedure via angular scaling is summarized in **Algorithm 1**. In the prediction stage, we use the learned  $w$  and  $b$  to update the calibrated similarity  $s'$  and the threshold  $\tau'$ , and then update the predictive confidence according to Eq. (3).

Now, we briefly explain why the angular scaling calibration ensures that the model maintains the prediction accuracy. Firstly, let  $\tau$  denote the uncalibrated threshold, and we are given the positive pair  $(X_p, Z_p)$  and negative pair  $(X_n, Z_n)$ , and their features are  $(x_p, x_p)$  and  $(x_n, z_n)$ , respectively. It is clearly that  $s(x_n, z_n) < \tau \leq s(x_p, z_p)$ , and since  $\arccos$  decreases monotonically in the interval  $[-1, 1]$ , we have:  $\theta_n > \theta_\tau \geq \theta_p$ . We then use  $w, b$  to adjust the angle between the two feature vectors. Because  $w > 0$ , we have  $\theta'_n > \theta'_\tau \geq \theta'_p$ , and  $\theta'_n, \theta'_\tau, \theta'_p \in [0, \pi]$  are satisfied. Likewise, we can also conclude  $\cos(\theta'_n) < \cos(\theta'_\tau) \leq \cos(\theta'_p)$ . Hence, it can be concluded that  $s'(x_n, z_n) < \tau' \leq s'(x_p, z_p)$ . This indicates that our proposed ASC learns to calibrate the predictive confidence while maintaining the verification accuracy.

To evaluate the calibration performance of our method for face and kinship verification, we use ECE (Expected Calibration Error) [48] as a metric. ECE is defined as the weighted average difference across bins between the expected accuracy and the predictive confidence:

---

**Algorithm 1** Angular Scaling Calibration (ASC)

---

**Input:** Recalibration set  $D_c = \{(X_i, Z_i), y_i\}_{i=1}^N$ .

**Output:** Calibration parameters  $w, b$ .

Set  $w = 1, b = 0$ ;

Compute the similarity set  $S_c$  of feature pairs

$$S_c = \{s(x_i, z_i)\}_{i=1}^N;$$

Compute the angle set  $\theta_c$  according to Eq.(4);

**while** not converged **do**

1. Update the angle set according to Eq. (5);

2. Update the similarity set according to Eq. (6);

3. Update  $w, b$  by optimizing the objective (8);

**end**

**return**  $w, b$

---

$$ECE = \sum_{m=1}^M \frac{|B_m|}{n} |acc(B_m) - conf(B_m)| \quad (9)$$

where  $B_m$  represents all predictions fall in the  $m$ th bin,  $M$  denotes the number of bins for partition of the confidence interval  $[0.5, 1]$ ,  $n$  is the total number of samples,  $acc(B_m)$  and  $conf(B_m)$  are the accuracy and confidence of  $m$ th bin, calculated by Eq. (10) and Eq. (11), respectively.

$$acc(B_m) = \frac{1}{|B_m|} \sum_{i \in B_m} 1(g(s_i, \tau) = y_i) \quad (10)$$

$$conf(B_m) = \frac{1}{|B_m|} \sum_{i \in B_m} c(s_i, \tau) \quad (11)$$

In general, there are two schemes towards bins partition [49]: one is to use equal-size interval partition, that is, the size of each bin is equal to  $1/2M$ , and the other is that each interval contains an equal number of samples. Note that a well-calibrated verification model often has a small ECE. Specifically, when the accuracy of each bin is equal to its confidence, the ECE of the model will be zero, indicating that it is perfectly calibrated.

#### IV. EXPERIMENTS

To validate the effectiveness of our proposed method for face and kinship verification, we conduct extensive experiments on four face and kinship datasets, including FIW, KinFaceW, LFW, and IJB-C. In this section, we will report the accuracy, the mean confidence, and the ECE before and after calibration on these datasets, and the experimental analysis are also present in detail.

##### A. Datasets and Experimental Settings

1) *FIW* [50]: FIW (Families In the Wild) [15], [50]–[52] is the largest visual kinship recognition dataset to date, consisting of over 13,000 facial images from 1000 families, with 11 pairwise kin relationships that can be divided into three sub-groups: siblings type (i.e., sister-sister, brother-brother, and sister-brother), parent-child type (i.e., father-son, father-daughter, mother-son, and mother-daughter), and grandparent-grandchild type (i.e., grandfather-grandson, grandfather-granddaughter, grandmother-grandson, and grandmother-granddaughter). The FIW is a challenging dataset because all the images are captured in the wild with partial occlusion and large variations in background, pose, expression, illumination, and so on.

InfoNCE [53], Triplet [9], Softmax [7], and ArcFace [14] are four widely-used losses in face and kinship verification tasks. We first use four loss functions to train models with different backbones pre-trained on the MS-celeb-1M [54]. We follow the data partitioning and evaluation protocol of RFIW 2021 [55]. To be more specific, we employ RetinaFace [56] for face alignment and the sample is cropped into  $112 \times 112$  pixels. SGD is used as the optimizer with a momentum of 0.9 and a learning rate of 0.0001.

TABLE I  
ACCURACY (%) AND MISCALIBRATION (%) PERFORMANCE OF DIFFERENT MODELS ON FIW [50]

Loss	Model	Accuracy												ECE
		SS	BB	SIBS	FD	MD	FS	MS	GFGD	GMGD	GFGS	GMGS	AVG	
InfoNCE	ResNet101	82.84	82.06	80.32	76.69	80.59	82.81	76.47	78.10	71.38	71.02	60.34	80.19	22.85
	ResNet50	79.00	74.81	75.92	71.82	74.15	78.60	72.10	73.36	70.26	63.67	61.45	75.01	16.51
	ResNet34	76.49	73.46	72.99	70.60	72.42	75.88	69.23	67.27	62.83	62.86	56.98	72.87	12.72
	VGG16	67.20	66.32	62.27	61.61	63.93	66.90	62.08	67.95	61.71	63.67	56.98	64.68	5.97
Triplet	ResNet101	80.49	79.50	78.79	73.34	79.04	80.53	74.34	77.88	77.32	68.98	59.22	77.94	20.93
	ResNet50	78.63	75.80	75.92	72.51	74.05	76.49	67.17	68.40	66.17	66.94	55.31	74.18	16.97
	ResNet34	75.17	73.95	71.29	72.26	71.03	76.26	69.39	69.75	64.68	62.04	59.78	72.86	10.46
	VGG16	66.14	64.80	64.32	63.76	62.13	67.01	64.02	65.69	68.03	66.53	50.84	64.65	7.87
ArcFace	ResNet101	80.23	79.36	79.38	75.62	77.52	81.19	73.54	76.75	75.84	71.02	61.45	78.02	19.39
	ResNet50	76.53	73.13	73.23	72.79	73.63	78.20	70.11	65.91	57.25	71.43	63.13	73.87	16.00
	ResNet34	74.67	74.06	70.94	71.12	71.00	75.66	67.25	64.55	62.83	58.37	61.45	72.16	10.04
	VGG16	67.98	67.11	61.86	60.86	63.93	68.00	61.60	61.63	65.43	55.92	58.10	64.83	7.69
Softmax	ResNet101	78.51	76.60	75.57	75.48	76.64	81.28	76.57	73.81	67.66	68.98	65.92	77.25	16.24
	ResNet50	75.90	75.21	73.29	69.57	73.49	78.06	70.48	66.37	60.97	77.14	64.25	73.74	15.77
	ResNet34	76.34	74.18	72.47	70.76	72.76	76.75	68.43	65.46	64.31	60.00	59.22	73.06	8.90
	VGG16	67.76	67.80	61.45	61.75	64.35	66.32	60.59	60.05	68.40	56.73	56.42	64.71	5.40

2) *KinFaceW* [16]: The *KinFaceW-I* and *KinFaceW-II* datasets are widely used kinship datasets comprised of Internet-collected images of public figures and celebrities. The two datasets contain four kin relations: Father-Son, Father-Daughter, Mother-Son, and Mother-Daughter. For these four kin relations, *KinFaceW-I* has 156, 134, 116, and 127 pairs of images with kin relationship. In *KinFaceW-II*, there are 250 pairs of images for each relationship. *KinFaceW-I* differs from *KinFaceW-II* in that, in most cases, the face pairs in the former dataset are from distinct photos while those in the latter one are from the same photos. Each image in the two datasets is aligned and resized into  $64 \times 64$  for feature extraction.

We evaluate two traditional and one deep-learning kinship verification methods on the *KinFaceW* datasets, including: 1) NRML (LBP) [16]: for each face image, we extract 3776-dimensional uniform pattern LBP features to kinship verification. 2) NRML (HOG) [16]: first, we partition each image into non-overlapping blocks. Then, we extract a 9-dimensional HOG feature for each block and concatenate them to generate a 2880-dimensional feature vector. 3) InfoNCE (ResNet18): we use InfoNCE loss to fine-tune a ResNet-18 model pre-trained on the MS1MV2 [14]. More specifically, the model is optimized using SGD, and the temperature parameter is set to 0.1. In this experiment, we use a five-fold cross-validation strategy in an image-unrestricted setting.

3) *LFW* [57], [58]: *LFW* contains 13,233 face images collected from 5,749 individuals, of which 1,680 have 2 or more face images.

We use CASIA-WebFace [59] as the training set to train networks of different depths with the ArcFace loss, and evaluate the verification performance of these models on the *LFW* dataset. In the experiments, we set the initial learning rate and momentum of the SGD optimizer to 0.1 and 0.9. We calibrate the confidence of the four models using ASC in the 10-fold cross-validation scheme. In addition, the maximum number of iterations and the learning rate for ASC are set to 1000 and 0.01, respectively.

4) *IJB-C* [60]: *IJB-C* (IARPA Janus Benchmark-C) dataset contains 31,334 images and 11,779 videos captured under unconstrained condition from 3,531 subjects. There are a total of 23,124 templates, with 19,557 positive matches and 15,638,932 negative matches to enable performance evaluations at low FAR.

In this experiment, we adopt the 1:1 Mixed Verification protocol, that is, a single feature vector was constructed by taking a weighted average of the frames in the template, so that all frames in a video belonging to the same subject have the same cumulative weight as a single still image. We perform face verification on the *IJB-C* dataset using different deep models trained on the MS1MV2 [14] with the ArcFace loss and the Triplet loss functions. To perform confidence estimation and calibration, we use five-fold cross-validation with stratified sampling of positive and negative samples, with four of the folds being the recalibration set and the remaining one being the test set.

## B. Experimental Results on FIW

In Table I, we show the verification accuracy, the weighted average accuracy, and the ECE on FIW dataset for different models and losses. From these results, we make the observations as below:

- 1) For all four loss functions, models with deeper architecture have better feature representation abilities. However, we also observe that increasing depth lead to a negative influence on model calibration.
- 2) Compared with Softmax and ArcFace loss, InfoNCE and Triplet loss achieve better verification accuracy. Especially as the model gets deeper, the performance improvement will be more noticeable; however the calibration error will increase.
- 3) ArcFace loss leverages the angular margin penalty to enforce extra intra-class compactness and inter-class discrepancy, achieving better verification performance with larger calibration error than Softmax loss.

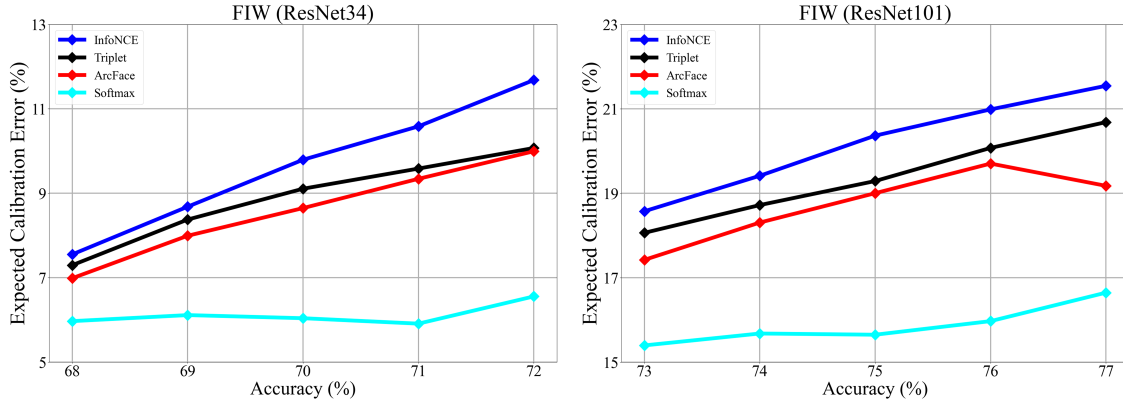


Fig. 3. The trend of verification accuracy (%) vs. ECE (%) of different verification models during training on FIW [50].

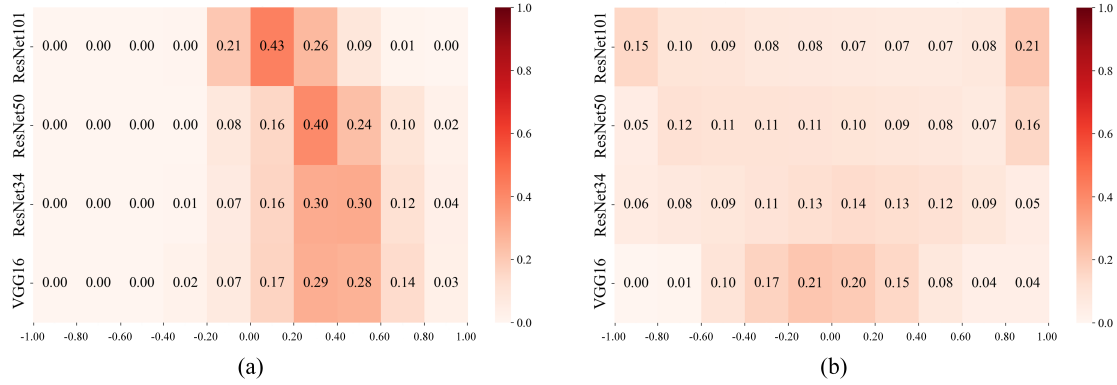


Fig. 4. Similarity distributions before calibration (a) and after calibration with ASC (b). From top to bottom are results of ResNet101, ResNet50, ResNet34, and VGG16, respectively.

In Fig. 3, we plot the accuracy-calibration during the training process of ResNet34 and ResNet101, intuitively showing the trend of the model’s ECE and verification accuracy with four different loss functions. It can be seen that the ECE of both models (ResNet34 and ResNet101) generally increase with the verification accuracy of the models. Also, if the model uses a loss that optimizes the feature representation, like InfoNCE or Triplet loss, the model has a larger ECE with the same accuracy.

In addition, we conduct experiments on the FIW dataset to evaluate the effects of the angular scaling calibration. Table II shows the ECE and thresholds before and after calibration. Specifically, we adopt LBFGS [61] as the calibration optimizer with a learning rate of 0.01 and a maximum number of iterations of 1000. The calibrated thresholds and calibration parameters ( $w$  and  $b$ ) are used to evaluate ECE on the test data.

From Table II, we observe that our ASC achieves good calibration on different models (loss functions). It is also found that the calibrated threshold tends to 0, so that positive and negative pairs are equally divided in the cosine similarity interval.

Fig. 4 plots the cosine similarity distribution for different models with InfoNCE loss before and after calibration on the

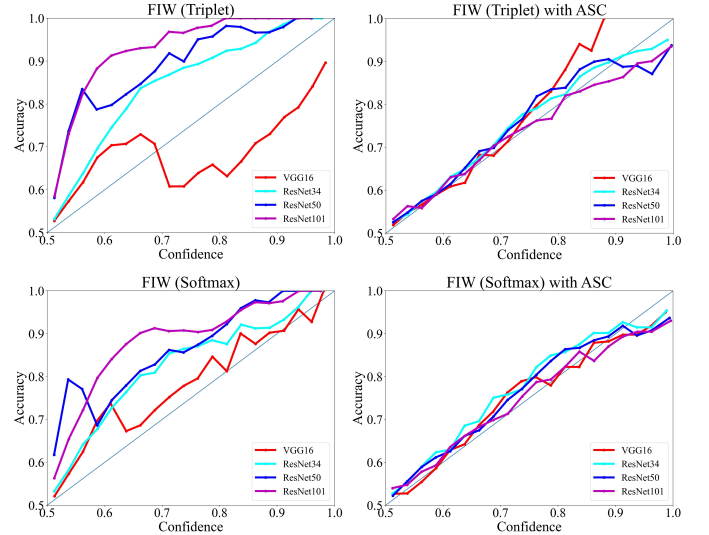


Fig. 5. Calibration plots of different models before and after calibration (with ASC) on FIW [50].

FIW dataset. We observe that the similarity before calibration is distributed over a smaller interval, leading to poor calibration, whereas the similarity after calibration is distributed



TABLE II  
CALIBRATION (%) PERFORMANCE OF DIFFERENT MODELS BEFORE AND AFTER CALIBRATION (WITH ASC) ON FIW [50]

Loss	Model	ECE	ECE w/ ASC	$\tau$	$\tau$ w/ ASC
InfoNCE	ResNet101	22.85	2.08	0.13	-0.01
	ResNet50	16.51	1.81	0.32	-0.03
	ResNet34	12.72	2.11	0.37	0.02
	VGG16	5.97	1.39	0.39	0.01
Triplet	ResNet101	20.93	2.83	0.11	0.02
	ResNet50	16.97	2.83	0.32	-0.07
	ResNet34	10.46	1.87	0.26	0.06
	VGG16	7.87	1.54	0.71	0.08
ArcFace	ResNet101	19.39	2.62	0.13	0.07
	ResNet50	16.00	2.45	0.39	-0.09
	ResNet34	10.04	3.40	0.14	-0.02
	VGG16	7.69	2.90	0.20	-0.07
Softmax	ResNet101	16.24	2.79	0.13	-0.04
	ResNet50	15.77	2.80	0.64	-0.05
	ResNet34	8.90	3.56	0.17	-0.01
	VGG16	5.40	1.81	0.37	0.01

uniformly over different similarity levels.

Fig. 5 is the accuracy-confidence plots of different models with Triplet loss and Softmax loss on the FIW dataset before and after calibration. The plots also show how well the predictive confidence is calibrated via angular scaling on all models, where perfect calibration corresponds to the line  $y = x$ . We can see that our ASC is able to obtain the well-calibrated predictions, as the recalibrated confidence correctly reflects the prediction accuracy.

Table III summarizes the average verification accuracy, average confidence before and after calibration of different models on three sub-groups of FIW. It can be seen that the confidence before calibration is significantly lower or higher than the actual verification accuracy, while the recalibrated confidence well matches the true accuracy of the model. Therefore, verification models calibrated by ASC can provide a reliable confidence estimation to support decision-making in face and kinship verification systems.

### C. Experimental Results on KinFaceW

In Table IV, we report the accuracy, the mean confidence, and the ECE before and after calibration on KinFaceW-I and KinFaceW-II datasets. We observe that models on the kin relationships (FS, MD) of same gender have higher verification accuracy and confidence than those of different gender (FD, MS), but the gain in accuracy is more significant. For NRML, the HOG achieves better verification accuracy and confidence than LBP, while it has a larger ECE. Compared to traditional verification methods, deep-learning methods perform less confidently, with the smallest confidence and largest ECE on most kin relationships. Besides, the accuracy is randomly distributed over the bins due to the small size of the KinFaceW dataset and limited number of data samples in each bin. However, the models calibrated by our ASC consistently show improved calibration performance in terms of both ECE and mean ECE.

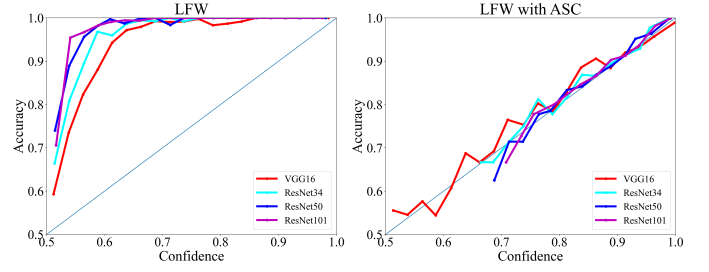


Fig. 6. Calibration plots of different models before and after calibration (with ASC) on LFW [57].

### D. Experimental Results on LFW

To further evaluate our method on face verification task, we also conduct experiments on the LFW dataset. As can be seen from Table V, deeper architectures may achieve better verification accuracy, but the calibration performance gets worse, which has also been demonstrated on both FIW and LFW. Moreover, Fig. 6 plots the correlation between the confidence and accuracy of the four models before and after calibration. We observe that ASC is helpful to improve the calibration of all four models. Due to the high accuracy of ResNet34, ResNet50, and ResNet101 on the LFW dataset, the calibration methods tend to map the predictive confidence to a high-level to match the expected accuracy. However, as shown in Fig. 6, the calibrated confidence of all four models does not degenerate to a constant solution, and instead it is well matched to the prediction accuracy of different levels.

### E. Experimental Results on IJB-C

We present in Table VI the threshold  $\tau$ , the TAR (True Accept Rate), the accuracy, the mean confidence, and the ECE before calibration on IJB-C dataset. The threshold increases as the FAR (False Accept Rate) drops from  $1e-2$  to  $1e-4$ , resulting in lower TAR and ECE. Also, it can be seen that the verification accuracy on all groups is above 99.7 %. Four groups of experiments show that ECE decreases with decreasing TAR, which is consistent with the correlation between ECE and accuracy. In the experiment, deeper model also gets larger ECE when achieving a better TAR, which is in line with the observations from previous experiments. Moreover, evaluating the effect of the loss function on the ECE reveals that the ResNet50 trained with the Triplet loss has a larger ECE than the model trained with ArcFace, even surpassing the ResNet101 model trained with ArcFace.

Table VII presents the accuracy, the mean confidence, and the ECE with ASC on the IJB-C datasets. The calibrated confidence is closer to the true accuracy, and the ECE is closer to zero. It shows that our proposed ASC yields good calibration performance for models with varying numbers of layers and loss functions, and it still keeps a small calibrator error even when the threshold changes.

### F. Comparison with Previous Post-calibration Methods

To validate the superiority of our ASC for confidence calibration in face and kinship verification, two widely used

TABLE III  
ACCURACY (%) AND CONFIDENCE (%) OF DIFFERENT MODELS BEFORE AND AFTER CALIBRATION (WITH ASC) ON DIFFERENT AGE GROUPS OF FIW [50]

Model	BB, SS, SIBS			FS, MS, FD, MD			GFGS, GMGS, GF GD, GMGD		
	Conf.	Conf. w/ ASC	Acc.	Conf.	Conf. w/ ASC	Acc.	Conf.	Conf. w/ ASC	Acc.
ResNet101	58.20	81.98	79.80	56.71	78.50	77.01	55.78	75.25	72.89
ResNet50	59.02	75.83	76.91	56.41	71.68	72.89	54.49	67.66	65.49
ResNet34	63.10	72.88	74.12	62.02	71.09	72.44	60.31	66.52	65.32
VGG16	70.34	64.11	65.26	69.20	63.63	64.29	67.86	63.22	64.08

TABLE IV  
ACCURACY (%), CONFIDENCE (%), AND ECE (%) OF DIFFERENT MODELS BEFORE AND AFTER CALIBRATION (WITH ASC) ON KINFACEW [16]

Dataset	Methods		FS			FD			MS			MD			Mean		
			Acc.	Conf.	ECE	Acc.	Conf.	ECE	Acc.	Conf.	ECE	Acc.	Conf.	ECE	Acc.	Conf.	ECE
KFW-I	NRML (LBP)	w/o ASC	81.43	57.01	27.03	69.42	55.40	19.24	67.23	55.94	18.04	72.87	56.08	19.48	72.74	56.11	20.95
		w/ ASC		79.94	1.97		68.43	1.39		64.64	2.49		71.05	2.70		71.02	2.14
	NRML (HOG)	w/o ASC	83.68	57.52	25.91	74.64	56.88	19.35	71.56	56.32	20.26	79.96	57.16	23.69	77.46	56.97	22.30
		w/ ASC		81.10	3.24		72.20	4.19		68.40	3.98		76.02	6.95		74.43	4.59
	InfoNCE (ResNet18)	w/o ASC	83.34	55.24	27.29	82.88	54.99	27.75	81.01	54.86	25.17	85.04	55.93	28.31	83.07	55.26	27.13
		w/ ASC		82.03	1.47		81.50	1.86		79.13	1.97		83.91	1.25		81.64	1.64
KFW-II	NRML (LBP)	w/o ASC	79.20	54.96	24.16	71.60	54.53	18.34	72.20	54.51	18.90	68.40	54.70	16.10	72.85	54.68	19.38
		w/ ASC		78.65	1.22		70.88	1.57		71.82	1.67		67.25	1.67		72.15	1.53
	NRML (HOG)	w/o ASC	80.80	55.75	24.90	72.80	55.14	19.16	74.80	55.41	20.57	70.40	55.24	18.48	74.70	55.39	20.78
		w/ ASC		79.76	1.06		72.24	1.86		74.27	1.68		68.82	1.89		73.77	1.62
	InfoNCE (ResNet18)	w/o ASC	84.00	55.37	28.13	78.20	54.50	23.20	82.20	55.15	26.55	84.00	55.16	28.34	82.10	55.05	26.56
		w/ ASC		83.48	0.60		78.16	0.81		80.55	1.54		83.17	1.06		81.34	1.00



Fig. 7. Visualization of confidence calibration by our ASC method. From top to bottom are examples from FIW, LFW, KinFaceW-I, and KinFaceW-II, respectively. The captions below each sample pair show the confidence adjustment before and after calibration. For better visualization, sample pairs with different confidence levels are shown in three groups: **low** confidence (a), **medium** confidence (b), and **high** confidence (c).

TABLE V  
ACCURACY (%) AND CONFIDENCE CALIBRATION (%) OF DIFFERENT  
MODELS BEFORE AND AFTER CALIBRATION (WITH ASC) ON LFW [57]

Model	Acc.	Conf.	Conf. w/ ASC	ECE	ECE w/ ASC
ResNet101	99.55	70.65	98.79	28.48	0.78
ResNet50	99.23	71.68	98.33	27.84	0.93
ResNet34	98.88	73.14	97.81	25.43	1.13
VGG16	93.57	70.89	93.31	24.67	1.54

post-calibration methods are chosen for performance comparison: Histogram binning [62] and Isotonic regression [63]. While there are some other post-calibration methods, such as Temperature scaling [40], Platt scaling [64], Bayesian binning [48], and Matrix and vector scaling, they cannot be directly applied to confidence calibration for face and kinship verification tasks. For fair comparison, we adopt the same experimental setting for all compared methods.

**Histogram binning** is a non-parametric calibration method. In this paper, Histogram binning firstly divide the cosine similarity score  $s$  evenly into  $M$  bins  $B_1, B_2, \dots, B_M$ , with bin boundaries  $-1 = a_1 < a_2 < \dots < a_M < a_{M+1} = 1$ , where the bin  $B_m$  refers to  $(a_m, a_{m+1}]$ . We assign each  $B_m$  a calibrated score  $\eta_m$ , which is optimized by:

$$\arg \min_{\eta_1, \dots, \eta_M} \sum_{m=1}^M \sum_{i=1}^N 1(a_m < s_i \leq a_{m+1})(\eta_m - y_i)^2 \quad (12)$$

where  $s_i, y_i$  are uncalibrated similarity score and the label of the  $i$ th sample pair, respectively. Once the  $i$ th sample falls into bin  $B_m$ , its calibrated similarity will be set to  $\eta_m$ . Additionally, the threshold  $\tau'$  is updated with  $\eta_t$ , where  $\tau' \in (a_t, a_{t+1}]$ .

**Isotonic regression** is another commonly used non-parametric calibration method that can be used for similarity score calibration by learning a piecewise constant function  $f$ , that is,  $s' = f(s)$ , where  $f(s_i) \leq f(s_j)$  if  $s_i \leq s_j$ . The goal of Isotonic regression is to minimize the square loss of  $\sum_{i=1}^N (f(s_i) - y_i)^2$ , which is optimized to learn the boundaries and calibration scores of each interval. We employ PAVA [65] algorithm to optimize the function  $f$ , and the calibrated threshold  $\tau'$  is set to  $f(\tau)$ .

Table VIII shows the calibration of three alternative methods (ASC, Histogram binning, and Isotonic regression) on the FIW, KinFaceW, LFW, and IJB-C datasets, in terms of ECE metric. We observe that ASC achieves the best calibration performance in most cases. Our method is easy to implement, as it involves only two parameters to be optimized and they can be efficiently learned by most gradient-based optimizers.

### G. Visualization Analysis

In Fig. 7, confidence calibration on sampled pairs from four datasets are presented. We divide sample pairs into three groups according to the recalibrated confidence value: low confidence, medium confidence, and high confidence. As expected, the visualization results show that samples with low

confidence are usually accompanied by certain facial occlusions, pose variations, age discrepancies, or image blurring, whereas samples with high confidence tend to have the same pose, background, and illumination conditions. Consistent with the previous experiments, we observe that models usually make incorrect predictions on low-confidence samples and correct predictions on high-confidence samples. The samples with medium confidence usually have similar issues as those with low confidence, but the facial region is complete, so there is a higher probability that they can be correctly predicted by the face or kinship verification models. In addition, ASC has good calibration ability for those samples of over-confidence (the first row) and under-confidence (the second, third, and fourth rows), making the calibrated confidence close to the average accuracy. All in all, our proposed confidence calibration method via angular scaling does not require retraining of the verification model while still maintaining its verification performance.

## V. CONCLUSIONS

In this work, we propose a simple yet effective confidence measure for face and kinship verification tasks, allowing any off-the-shelf verification models to estimate the decision confidence in an efficient and flexible way. We further introduce a confidence calibration method using angular scaling for face and kinship verification tasks, which is retraining-free and accuracy-preserving. We perform comprehensive experiments on four widely used face and kinship verification datasets to investigate the calibration of popular face/kinship verification models, and the effectiveness of our ASC is validated in these experiments. Experimental comparisons with two popular post-calibration methods demonstrate that our ASC achieves superior calibration performance. In future work, incorporation of uncertainty modeling in confidence estimation and confidence calibration appears to be an interesting and promising direction in face and kinship verification.

## REFERENCES

- [1] S. Chopra, R. Hadsell, and Y. LeCun, "Learning a similarity metric discriminatively, with application to face verification," in *2005 IEEE Computer Society Conference on Computer Vision and Pattern Recognition (CVPR)*, vol. 1. IEEE, 2005, pp. 539–546.
- [2] R. Fang, K. D. Tang, N. Snavely, and T. Chen, "Towards computational models of kinship verification," in *2010 IEEE International conference on image processing*. IEEE, 2010, pp. 1577–1580.
- [3] W. Xie, J. Byrne, and A. Zisserman, "Inducing predictive uncertainty estimation for face recognition," in *Proceedings of the British Machine Vision Conference (BMVC)*, 2020.
- [4] J. Chang, Z. Lan, C. Cheng, and Y. Wei, "Data uncertainty learning in face recognition," in *Proceedings of the IEEE/CVF Conference on Computer Vision and Pattern Recognition*, 2020, pp. 5710–5719.
- [5] Y. Shi and A. K. Jain, "Probabilistic face embeddings," in *Proceedings of the IEEE/CVF International Conference on Computer Vision*, 2019, pp. 6902–6911.
- [6] Y. Zhang, C. Wang, and W. Deng, "Relative uncertainty learning for facial expression recognition," *Advances in Neural Information Processing Systems*, vol. 34, pp. 17 616–17 627, 2021.
- [7] Y. Taigman, M. Yang, M. Ranzato, and L. Wolf, "Deepface: Closing the gap to human-level performance in face verification," in *Proceedings of the IEEE conference on computer vision and pattern recognition*, 2014, pp. 1701–1708.

TABLE VI  
ACCURACY (%), CONFIDENCE (%), AND CALIBRATION (%) OF DIFFERENT MODELS BEFORE CALIBRATION ON IJB-C [60]

Loss	Model	FAR=1e-2					FAR=1e-4					AUC
		$\tau$	TAR	Acc.	Conf.	ECE	$\tau$	TAR	Acc.	Conf.	ECE	
ArcFace	ResNet101	0.03	97.17	99.92	65.54	34.89	0.22	93.92	99.94	70.76	29.64	99.25
	ResNet50	-0.17	96.69	99.92	68.62	31.36	0.09	90.16	99.93	75.47	23.97	99.25
	ResNet34	-0.20	96.02	99.89	71.99	27.98	0.02	90.56	99.93	77.56	21.93	99.24
Triplet	ResNet50	0.15	93.35	99.71	64.73	35.10	0.28	86.31	99.90	68.31	31.36	99.07

TABLE VII  
ACCURACY (%), CONFIDENCE (%), AND CALIBRATION (%) OF DIFFERENT MODELS AFTER CALIBRATION (WITH ASC) ON IJB-C [60]

Loss	Model	FAR=1e-2			FAR=1e-4		
		Acc.	Conf.	ECE	Acc.	Conf.	ECE
ArcFace	ResNet101	99.92	98.77	1.30	99.94	99.52	0.47
	ResNet50	99.92	98.80	1.18	99.93	99.46	0.53
	ResNet34	99.89	98.06	1.90	99.93	99.36	0.63
Triplet	ResNet50	99.71	97.72	2.24	99.90	97.95	2.19

- [8] Y. Sun, D. Liang, X. Wang, and X. Tang, "DeepID3: Face recognition with very deep neural networks," *arXiv preprint arXiv: 1502.00873*, 2015.
- [9] F. Schroff, D. Kalenichenko, and J. Philbin, "FaceNet: A unified embedding for face recognition and clustering," in *Proceedings of the IEEE conference on computer vision and pattern recognition*, 2015, pp. 815–823.
- [10] Y. Wen, K. Zhang, Z. Li, and Y. Qiao, "A discriminative feature learning approach for deep face recognition," in *European conference on computer vision*. Springer, 2016, pp. 499–515.
- [11] W. Liu, Y. Wen, Z. Yu, and M. Yang, "Large-margin softmax loss for convolutional neural networks," *arXiv preprint arXiv: 1612.02295*, 2016.
- [12] W. Liu, Y. Wen, Z. Yu, M. Li, B. Raj, and L. Song, "Sphereface: Deep hypersphere embedding for face recognition," in *Proceedings of the IEEE conference on computer vision and pattern recognition*, 2017, pp. 212–220.
- [13] H. Wang, Y. Wang, Z. Zhou, X. Ji, D. Gong, J. Zhou, Z. Li, and W. Liu, "Cosface: Large margin cosine loss for deep face recognition," in *Proceedings of the IEEE conference on computer vision and pattern recognition*, 2018, pp. 5265–5274.
- [14] J. Deng, J. Guo, N. Xue, and S. Zafeiriou, "Arcface: Additive angular margin loss for deep face recognition," in *Proceedings of the IEEE/CVF*

TABLE VIII  
COMPARISON OF ECE (%) FOR DIFFERENT POST-CALIBRATION METHODS ON FOUR DATASETS

Dataset	Loss (Method)	Model (Feature)	Uncalibrated	Histogram binning [62]	Isotonic regression [63]	ASC
FIW	InfoNCE	ResNet101	22.85	2.47	2.51	<b>2.08</b>
		ResNet50	16.51	<b>1.57</b>	1.62	1.81
		ResNet34	12.72	2.89	2.60	<b>2.11</b>
		VGG16	5.97	2.14	2.17	<b>1.39</b>
	Triplet	ResNet101	20.93	<b>1.22</b>	1.36	2.83
		ResNet50	16.97	2.83	<b>2.82</b>	2.83
		ResNet34	10.46	2.80	2.57	<b>1.87</b>
		VGG16	7.87	<b>1.51</b>	4.70	1.54
	ArcFace	ResNet101	19.39	3.14	2.95	<b>2.62</b>
		ResNet50	16.00	4.75	4.78	<b>2.45</b>
		ResNet34	10.04	3.45	3.76	<b>3.40</b>
		VGG16	7.69	1.66	<b>1.40</b>	2.90
	Softmax	ResNet101	16.24	1.37	<b>1.20</b>	2.79
		ResNet50	15.77	2.92	2.85	<b>2.80</b>
		ResNet34	8.90	3.82	3.65	<b>3.56</b>
		VGG16	5.40	2.05	1.84	<b>1.81</b>
KinFaceW-I	NRML	LBP	20.95	<b>1.90</b>	3.06	2.14
		HOG	22.30	4.98	<b>4.56</b>	4.59
	InfoNCE	ResNet18	27.13	1.69	2.92	<b>1.64</b>
KinFaceW-II	NRML	LBP	19.38	<b>1.08</b>	1.34	1.53
		HOG	20.78	2.22	<b>1.37</b>	1.62
	InfoNCE	ResNet18	26.56	2.35	2.22	<b>1.00</b>
LFW	ArcFace	ResNet101	28.48	1.22	<b>0.16</b>	0.78
		ResNet50	27.84	0.98	<b>0.70</b>	0.93
		ResNet34	25.43	2.35	1.76	<b>1.13</b>
		VGG16	24.67	2.56	1.58	<b>1.54</b>
IJB-C	ArcFace	ResNet101	29.64	1.18	0.97	<b>0.47</b>
		ResNet50	23.97	1.49	1.00	<b>0.53</b>
		ResNet34	21.93	1.72	1.14	<b>0.63</b>
	Triplet	ResNet50	31.36	2.24	<b>2.07</b>	2.19



- conference on computer vision and pattern recognition, 2019, pp. 4690–4699.
- [15] J. P. Robinson, M. Shao, and Y. Fu, “Survey on the analysis and modeling of visual kinship: A decade in the making,” *IEEE Transactions on Pattern Analysis and Machine Intelligence*, vol. 44, no. 8, pp. 4432–4453, 2021.
  - [16] J. Lu, X. Zhou, Y.-P. Tan, Y. Shang, and J. Zhou, “Neighborhood repulsed metric learning for kinship verification,” *IEEE transactions on pattern analysis and machine intelligence*, vol. 36, no. 2, pp. 331–345, 2013.
  - [17] H. Yan, J. Lu, W. Deng, and X. Zhou, “Discriminative multimetric learning for kinship verification,” *IEEE Transactions on Information forensics and security*, vol. 9, no. 7, pp. 1169–1178, 2014.
  - [18] X. Zhou, Y. Shang, H. Yan, and G. Guo, “Ensemble similarity learning for kinship verification from facial images in the wild,” *Information Fusion*, vol. 32, pp. 40–48, 2016.
  - [19] J. Hu, J. Lu, L. Liu, and J. Zhou, “Multi-view geometric mean metric learning for kinship verification,” in *2019 IEEE international conference on image processing (ICIP)*. IEEE, 2019, pp. 1178–1182.
  - [20] M. Xu and Y. Shang, “Kinship measurement on face images by structured similarity fusion,” *IEEE Access*, vol. 4, pp. 10 280–10 287, 2016.
  - [21] X. Zhou, H. Yan, and Y. Shang, “Kinship verification from facial images by scalable similarity fusion,” *Neurocomputing*, vol. 197, pp. 136–142, 2016.
  - [22] S. Wang, J. P. Robinson, and Y. Fu, “Kinship verification on families in the wild with marginalized denoising metric learning,” in *2017 12th IEEE international conference on automatic face & gesture recognition (FG 2017)*. IEEE, 2017, pp. 216–221.
  - [23] J. Lu, J. Hu, and Y.-P. Tan, “Discriminative deep metric learning for face and kinship verification,” *IEEE Transactions on Image Processing*, vol. 26, no. 9, pp. 4269–4282, 2017.
  - [24] X. Qin, D. Liu, and D. Wang, “Social relationships classification using social contextual features and svdd-based metric learning,” *Applied Soft Computing*, vol. 77, pp. 344–355, 2019.
  - [25] Q. Duan, L. Zhang, and W. Zuo, “From face recognition to kinship verification: An adaptation approach,” in *Proceedings of the IEEE international conference on computer vision workshops*, 2017, pp. 1590–1598.
  - [26] S. Wang, Z. Ding, and Y. Fu, “Cross-generation kinship verification with sparse discriminative metric,” *IEEE transactions on pattern analysis and machine intelligence*, vol. 41, no. 11, pp. 2783–2790, 2018.
  - [27] N. Kohli, D. Yadav, M. Vatsa, R. Singh, and A. Noore, “Deep face-representation learning for kinship verification,” *Deep learning in biometrics*, p. 127, 2018.
  - [28] K. Zhang, Y. Huang, C. Song, H. Wu, L. Wang, and S. M. Intelligence, “Kinship verification with deep convolutional neural networks,” *British machine vision conference*. BMVA Press, 2015.
  - [29] X. Zhou, K. Jin, M. Xu, and G. Guo, “Learning deep compact similarity metric for kinship verification from face images,” *Information Fusion*, vol. 48, pp. 84–94, 2019.
  - [30] G.-N. Dong, C.-M. Pun, and Z. Zhang, “Kinship verification based on cross-generation feature interaction learning,” *IEEE Transactions on Image Processing*, vol. 30, pp. 7391–7403, 2021.
  - [31] J. Hu, J. Lu, Y.-P. Tan, J. Yuan, and J. Zhou, “Local large-margin multi-metric learning for face and kinship verification,” *IEEE Transactions on Circuits and Systems for Video Technology*, vol. 28, no. 8, pp. 1875–1891, 2017.
  - [32] Z. Wei, M. Xu, L. Geng, H. Liu, and H. Yin, “Adversarial similarity metric learning for kinship verification,” *IEEE Access*, vol. 7, pp. 100 029–100 035, 2019.
  - [33] H. Zhang, X. Wang, and C.-C. J. Kuo, “Deep kinship verification via appearance-shape joint prediction and adaptation-based approach,” in *2019 IEEE international conference on image processing (ICIP)*. IEEE, 2019, pp. 3856–3860.
  - [34] A. Goyal and T. Meenpal, “Robust discriminative feature subspace analysis for kinship verification,” *Information Sciences*, vol. 578, pp. 507–524, 2021.
  - [35] J. Zhu, M. Shao, C. Xia, H. Pan, and S. Xia, “Adversarial attacks on kinship verification using transformer,” in *2021 16th IEEE International Conference on Automatic Face and Gesture Recognition (FG 2021)*. IEEE, 2021, pp. 1–8.
  - [36] S. Ozkan and A. Ozkan, “Kinshipgan: Synthesizing of kinship faces from family photos by regularizing a deep face network,” in *2018 25th IEEE international conference on image processing (ICIP)*. IEEE, 2018, pp. 2142–2146.
  - [37] P. Gao, J. Robinson, J. Zhu, C. Xia, M. Shao, and S. Xia, “DNA-Net: Age and gender aware kin face synthesizer,” in *2021 IEEE International Conference on Multimedia and Expo (ICME)*. IEEE, 2021, pp. 1–6.
  - [38] W. Li, Y. Zhang, K. Lv, J. Lu, J. Feng, and J. Zhou, “Graph-based kinship reasoning network,” in *2020 IEEE international conference on multimedia and expo (ICME)*. IEEE, 2020, pp. 1–6.
  - [39] M. Huber, P. Terhörst, F. Kirchbuchner, N. Damer, and A. Kuijper, “Stat-ing comparison score uncertainty and verification decision confidence towards transparent face recognition,” *arXiv preprint arXiv: 2210.10354*, 2022.
  - [40] C. Guo, G. Pleiss, Y. Sun, and K. Q. Weinberger, “On calibration of modern neural networks,” in *International conference on machine learning*. PMLR, 2017, pp. 1321–1330.
  - [41] J. Choi, D. Chun, H. Kim, and H.-J. Lee, “Gaussian yolov3: An accurate and fast object detector using localization uncertainty for autonomous driving,” in *Proceedings of the IEEE/CVF International Conference on Computer Vision*, 2019, pp. 502–511.
  - [42] Alex Kendall, Vijay Badrinarayanan and Roberto Cipolla, “Bayesian segnet: Model uncertainty in deep convolutional encoder-decoder architectures for scene understanding,” in *Proceedings of the British Machine Vision Conference (BMVC)*, 2017, pp. 57.1–57.12.
  - [43] F. Warburg, M. Jørgensen, J. Civera, and S. Hauberg, “Bayesian triplet loss: Uncertainty quantification in image retrieval,” in *Proceedings of the IEEE/CVF International Conference on Computer Vision*, 2021, pp. 12 158–12 168.
  - [44] A. Taha, Y.-T. Chen, T. Misu, A. Shrivastava, and L. Davis, “Unsupervised data uncertainty learning in visual retrieval systems,” *arXiv preprint arXiv: 1902.02586*, 2019.
  - [45] A. Kendall and Y. Gal, “What uncertainties do we need in bayesian deep learning for computer vision?” *Advances in neural information processing systems*, vol. 30, 2017.
  - [46] Y. Gal and Z. Ghahramani, “Dropout as a bayesian approximation: Representing model uncertainty in deep learning,” in *international conference on machine learning*. PMLR, 2016, pp. 1050–1059.
  - [47] S. Khan, M. Hayat, S. W. Zamir, J. Shen, and L. Shao, “Striking the right balance with uncertainty,” in *Proceedings of the IEEE/CVF Conference on Computer Vision and Pattern Recognition*, 2019, pp. 103–112.
  - [48] M. P. Naeini, G. Cooper, and M. Hauskrecht, “Obtaining well calibrated probabilities using bayesian binning,” in *Twenty-Ninth AAAI Conference on Artificial Intelligence*, 2015.
  - [49] J. Nixon, M. W. Dusenberry, L. Zhang, G. Jerfel, and D. Tran, “Measuring calibration in deep learning,” in *CVPR Workshops*, vol. 2, no. 7, 2019.
  - [50] J. P. Robinson, M. Shao, Y. Wu, and Y. Fu, “Families in the wild (fiw) large-scale kinship image database and benchmarks,” in *Proceedings of the 24th ACM international conference on Multimedia*, 2016, pp. 242–246.
  - [51] J. P. Robinson, M. Shao, Y. Wu, H. Liu, T. Gillis, and Y. Fu, “Visual kinship recognition of families in the wild,” *IEEE Transactions on pattern analysis and machine intelligence*, vol. 40, no. 11, pp. 2624–2637, 2018.
  - [52] J. P. Robinson, Y. Yin, Z. Khan, M. Shao, S. Xia, M. Stopa, S. Timoner, M. A. Turk, R. Chellappa, and Y. Fu, “Recognizing families in the wild (rfiw): The 4th edition,” in *2020 15th IEEE International Conference on Automatic Face and Gesture Recognition (FG 2020)*. IEEE, 2020, pp. 857–862.
  - [53] T. Chen, S. Kornblith, M. Norouzi, and G. Hinton, “A simple framework for contrastive learning of visual representations,” in *International conference on machine learning*. PMLR, 2020, pp. 1597–1607.
  - [54] Y. Guo, L. Zhang, Y. Hu, X. He, and J. Gao, “Ms-celeb-1m: A dataset and benchmark for large-scale face recognition,” in *European conference on computer vision*. Springer, 2016, pp. 87–102.
  - [55] J. P. Robinson, C. Qin, M. Shao, M. A. Turk, R. Chellappa, and Y. Fu, “The 5th recognizing families in the wild data challenge: Predicting kinship from faces,” in *2021 16th IEEE International Conference on Automatic Face and Gesture Recognition (FG 2021)*. IEEE, 2021, pp. 01–07.
  - [56] J. Deng, J. Guo, E. Ververas, I. Kotsia, and S. Zafeiriou, “Retinaface: Single-shot multi-level face localisation in the wild,” in *Proceedings of the IEEE/CVF conference on computer vision and pattern recognition*, 2020, pp. 5203–5212.

- [57] G. B. Huang, M. Mattar, T. Berg, and E. Learned-Miller, "Labeled faces in the wild: A database for studying face recognition in unconstrained environments," in *Workshop on faces in 'Real-Life' Images: detection, alignment, and recognition*, 2008.
- [58] G. B. Huang and E. Learned-Miller, "Labeled faces in the wild: Updates and new reporting procedures," *Dept. Comput. Sci., Univ. Massachusetts Amherst, Amherst, MA, USA, Tech. Rep.*, vol. 14, no. 003, 2014.
- [59] D. Yi, Z. Lei, S. Liao, and S. Z. Li, "Learning face representation from scratch," *arXiv preprint arXiv: 1411.7923*, 2014.
- [60] B. Maze, J. Adams, J. A. Duncan, N. Kalka, T. Miller, C. Otto, A. K. Jain, W. T. Niggel, J. Anderson, J. Cheney *et al.*, "Iarpa janus benchmark-c: Face dataset and protocol," in *2018 international conference on biometrics (ICB)*. IEEE, 2018, pp. 158–165.
- [61] J. Nocedal, "Updating quasi-newton matrices with limited storage," *Mathematics of computation*, vol. 35, no. 151, pp. 773–782, 1980.
- [62] B. Zadrozny and C. Elkan, "Obtaining calibrated probability estimates from decision trees and naive bayesian classifiers," in *Proceedings of the Eighteenth International Conference on Machine Learning*, vol. 1. Citeseer, 2001, pp. 609–616.
- [63] Zadrozny, Bianca and Elkan, Charles, "Transforming classifier scores into accurate multiclass probability estimates," in *Proceedings of the eighth ACM SIGKDD international conference on Knowledge discovery and data mining*, 2002, pp. 694–699.
- [64] J. Platt *et al.*, "Probabilistic outputs for support vector machines and comparisons to regularized likelihood methods," *Advances in large margin classifiers*, vol. 10, no. 3, pp. 61–74, 1999.
- [65] J. De Leeuw, K. Hornik, and P. Mair, "Isotone optimization in R: pool-adjacent-violators algorithm (pava) and active set methods," *Journal of statistical software*, vol. 32, pp. 1–24, 2010.